



Thank you for downloading this document from the RMIT Research Repository.

The RMIT Research Repository is an open access database showcasing the research outputs of RMIT University researchers.

RMIT Research Repository: <http://researchbank.rmit.edu.au/>

Citation:

Davy, J, Fard, M, Dong, W and Loverde, J 2019, 'Empirical corrections for predicting the sound insulation of double leaf cavity stud building elements with stiffer studs', Journal of the Acoustical Society of America, vol. 145, no. 2, pp. 703-713

See this record in the RMIT Research Repository at:

<https://researchbank.rmit.edu.au/view/rmit:51447>

Version: Accepted Manuscript

Copyright Statement:

© 2019 Acoustical Society of America

Link to Published Version:

<https://dx.doi.org/10.1121/1.5089222>

PLEASE DO NOT REMOVE THIS PAGE

Empirical corrections for predicting the sound insulation of double leaf cavity stud building
elements with stiffer studs

John L. Davy^{ab}

Mohammad Fard

Royal Melbourne Institute of Technology (RMIT) University, GPO Box 2476, Melbourne,
Victoria 3001, Australia

Wayland Dong

John Loverde

Veneklasen Associates, 1711 Sixteenth Street, Santa Monica, CA 90404, United States of
America

Running Title: Sound insulation of cavity stud elements

^a Author to whom correspondence should be addressed. Electronic mail: john.davy@rmit.edu.au

^b Current address: CSIRO Infrastructure Technologies, Private Bag 10, Clayton South, Victoria
3169, Australia.

ABSTRACT

The experimentally determined normal incident mass-air-mass resonance frequency for a double leaf cavity stud building element is significantly greater than the theoretically predicted frequency for wood studs and steel studs manufactured from thicker sheet steel. This paper gives a method for calculating the effective mass-air-mass resonance frequency as the root mean square sum of the mass-air-mass resonance frequency and the resonance frequency of the first bending wave mode of the leaves between the studs. This calculation should use the isothermal mass-air-mass resonance frequency if the building element cavity contains porous sound absorbing material. If the cavity does not contain porous sound absorbing material, the usual adiabatic mass-air-mass resonance frequency should be used in the calculation. Because the exact boundary conditions of the building element leaves at the studs and the effective in situ damping are unknown, the paper gives empirical correction factors to determine the actual resonance frequency and the depth of the dip in the predicted sound insulation. This paper also gives empirically derived formulae for the line and point equivalent translational compliances of steel studs manufactured from different sheet steel gauges and compares them with formulae derived by other authors for the case of 25 gauge steel studs.

PACS numbers: 43.55.Rg, 43.55.Ti, 43.40.Rj, 43.20.Rz

I. INTRODUCTION

Theories for calculating the sound insulation of cavity stud walls predict that there will be a minimum or a change of slope at the normal incidence mass-air mass resonance frequency. However figure 6 in Davy (2009) with one experimental measurement for 13 mm gypsum plaster board on each side of the studs, and figure 6 in Davy (2010) with three experimental measurements for 16 mm gypsum plaster board on each side of the studs, both show that the dip in the measured sound insulation occurs at a higher frequency than the theoretically predicted normal incidence mass-air mass resonance frequency for the case of 90 mm rigid wood stud walls with porous sound absorbing material in the cavity.

Davy (2010) comments that “Note that the predicted mass-air-mass resonance frequency of about 80 Hz is significantly less than the measured mass-air-mass resonance frequencies of 125 or 160 Hz. This may be due to a structural resonance, which is not included in the theory described in this paper. Bradley and Birta (2001) showed that the sound insulation of wood stud exterior walls can be significantly degraded by a structural resonance if the two wall leaves are rigidly coupled by the wooden studs. They explained this structural resonance in terms of the analysis conducted by Lin and Garrelick (1977). The effects of this resonance can be reduced by structurally isolating the two wall leaves with resilient mounts. The frequency of the resonance is about double the calculated mass-air-mass resonance, and it reduces in frequency as the rigid stud spacing is increased and as the depth of the rigid studs is increased.”

“Bradley and Birta (2000) reported the results of laboratory sound insulation measurements on typical Canadian building facades. These measurements showed the structural resonance at 125

63 Hz. However, field measurements by Bradley *et al.* (2002) and Bradley (2002) with actual aircraft
64 noise showed little effect due to this structural resonance.”

65 Recently, Davy *et al.* (2018) also observed that the dip in the measured sound insulation
66 occurs at a higher frequency than the theoretically predicted normal incidence mass-air-mass
67 resonance frequency for cavity walls with one or two layers of 16 mm gypsum plaster board
68 screwed to both sides of steel studs made from sheet steel thicker than 25 gauge. This difference
69 in resonance frequency led to differences between the measured and predicted sound insulation of
70 up to 17.5 dB at 160 Hz. The differences between measured and predicted sound insulation in the
71 region of 160 Hz are much greater for a stud spacing of 406 mm than for a stud spacing of 610
72 mm. These observations prompted the research described in this paper.

73 The first objective of this paper is to offer a physical explanation of why the experimentally
74 observed effective mass-air-mass resonance frequency for cavity stud walls with stiffer studs is
75 significantly higher than the theoretically predicted normal incidence mass-air-mass resonance
76 frequency. The second objective is to provide formulae for the equivalent translational compliance
77 of stiffer steel studs for use in simple models for predicting the sound insulation of cavity stud
78 walls. The third objective is to point out that the isothermal speed of sound should be used for
79 wall cavities which are filled with porous sound absorbing material. Although this paper is not
80 able to present a fully developed prediction method, because it is not able to present equations for
81 deriving some of the empirical constants, it is hoped that it will draw other researchers’ attention
82 to this important but difficult problem.

83 Van den Wyngaert *et al.* (2018) review different theories for predicting the sound insulation
84 of cavity stud walls. Lin and Garrelick (1977) is the only paper that the authors are aware of which

has theoretically predicted the significant increase in the effective mass-air-mass resonance frequency which occurs with stiffer studs and they only considered wooden studs. Unfortunately, their dimensionless variables appear to disagree with the properties of the wall whose sound insulation they claimed to be calculating. Their use of the Fourier series method means that the actual physical reason for the increase in effective mass-air-mass resonance frequency is not obvious and they are unable to model the effects of the finite size of the wall.

Formulae for the equivalent translational compliance or stiffness of steel studs have only been provided for 25 gauge steel studs (Poblet-Puig *et al.*, 2009; Vigran, 2010a; Davy *et al.*, 2012; Hirakawa and Davy, 2015), except for a conference paper (Davy *et al.*, 2018). Narang (1993) and Davy *et al.* (2017) have provided experimental evidence for the use of the isothermal speed of sound in a wall cavity which is filled with sound absorbing material.

II. THEORY

The first bending mode between two adjacent studs of each wall leaf of a cavity stud wall is modelled as a linear harmonic oscillator. These two linear harmonic oscillators are coupled by the spring of the air cavity. The position, mass and stiffness of each linear harmonic oscillator are x_i , m_i and K_i respectively where $i = 1, 2$. The stiffness of the spring coupling the two linear harmonic oscillators is K_{12} . The system comprising the two coupled linear harmonic oscillators has kinetic energy T and potential energy V . Its Lagrangian is

$$L = T - V = m_1 \dot{x}_1^2 / 2 + m_2 \dot{x}_2^2 / 2 - K_1 x_1^2 / 2 - K_{12} (x_2 - x_1)^2 / 2 - K_2 x_2^2 / 2. \quad (1)$$

The Lagrangian equations of motion are

$$\frac{d}{dt} \left(\frac{\partial L}{\partial \dot{x}_i} \right) - \frac{\partial L}{\partial x_i} = 0 \text{ for } i = 1, 2, \quad (2)$$

where t is the time. Applying equations (2) to equation (1) gives

$$\begin{aligned} m_1 \ddot{x}_1 + (K_1 + K_{12})x_1 - K_{12}x_2 &= 0 \\ m_2 \ddot{x}_2 - K_{12}x_1 + (K_2 + K_{12})x_2 &= 0 \end{aligned} \quad (3)$$

To find the resonance angular frequencies of the two coupled linear harmonic oscillators, assume that

$$x_i = a_i \exp(j\omega t) \text{ for } i = 1, 2, \quad (4)$$

where a_i , $i = 1, 2$, are the complex amplitudes of the two coupled linear harmonic oscillators and ω is the angular frequency. This assumption gives

$$\begin{pmatrix} K_1 + K_{12} - \omega^2 m_1 & -K_{12} \\ -K_{12} & K_2 + K_{12} - \omega^2 m_2 \end{pmatrix} \begin{pmatrix} a_1 \\ a_2 \end{pmatrix} = \begin{pmatrix} 0 \\ 0 \end{pmatrix}. \quad (5)$$

Equation (5) can only be true for non-zero a_i , $i = 1, 2$, if the determinant of the matrix in equation (5) is zero. Thus

$$(K_1 + K_{12} - \omega^2 m_1)(K_2 + K_{12} - \omega^2 m_2) - K_{12}^2 = 0. \quad (6)$$

Dividing equation (6) by $m_1 m_2$ gives

$$(K_1/m_1 + K_{12}/m_1 - \omega^2)(K_2/m_2 + K_{12}/m_2 - \omega^2) - (K_{12}/m_1)(K_{12}/m_2) = 0. \quad (7)$$

Putting

$$f = \frac{\omega}{2\pi}, f_1 = \frac{1}{2\pi} \sqrt{\frac{K_1}{m_1}}, f_2 = \frac{1}{2\pi} \sqrt{\frac{K_2}{m_2}}, f_{a1} = \frac{1}{2\pi} \sqrt{\frac{K_{12}}{m_1}} \text{ and } f_{a2} = \frac{1}{2\pi} \sqrt{\frac{K_{12}}{m_2}}, \quad (8)$$

gives

$$(f^2 - f_1^2 - f_{a1}^2)(f^2 - f_2^2 - f_{a2}^2) - f_{a1}^2 f_{a2}^2 = 0. \quad (9)$$

Expanding this equation gives

$$f^4 + pf^2 + q = 0, \quad (10)$$

where

$$p = -(f_1^2 + f_2^2 + f_{a1}^2 + f_{a2}^2) \text{ and } q = f_1^2 f_2^2 + f_1^2 f_{a2}^2 + f_2^2 f_{a1}^2. \quad (11)$$

Thus, the resonance frequencies of the system comprising two coupled linear harmonic oscillators are

$$f_{\pm} = \sqrt{(-p \pm \sqrt{p^2 - 4q})/2}. \quad (12)$$

If $f_1 = f_2 = f_0$ and $f_{a1} = f_{a2} = f_a$ then equation (9) becomes

$$(f^2 - f_0^2)(f^2 - [f_0^2 + 2f_a^2]) = 0, \quad (13)$$

and its positive solutions give the two resonance frequencies of the coupled linear harmonic oscillators as

$$f_- = f_0 \text{ and } f_+ = \sqrt{f_0^2 + 2f_a^2}. \quad (14)$$

In the situation considered in this paper, the frequency f_i is the resonance frequency of the first bending mode of the i th wall leaf between two adjacent studs and f_{ai} is the normal incidence mass-air resonance frequency of the i th wall leaf and the air in the wall cavity.

The normal incidence mass-air resonance frequency f_{ai} of the i th wall leaf and the air in the wall cavity is

$$f_{ai} = \frac{1}{2\pi} \sqrt{\frac{\rho_0 c^2}{dm_i}}, \quad (15)$$

where ρ_0 is the density of air, m_i is the mass per unit area of the i th wall leaf, d is the width of the wall cavity and c is the speed of sound in air. This means that if $m = m_1 = m_2$ is the mass per unit area of each wall leaf, the second term under the square root in equation (14) is the square of the normal incidence mass-air-mass resonance frequency f_{mam} .

$$\sqrt{2f_a^2} = \frac{1}{2\pi} \sqrt{\frac{\rho_0 c^2}{d} \frac{(m+m)}{mm}} = \frac{1}{2\pi} \sqrt{\frac{\rho_0 c^2}{d} \frac{(m_1+m_2)}{m_1 m_2}} = f_{mam}, \quad (16)$$

Thus, when the wall leaves are the same, the lower resonance frequency f_- is the resonance frequency of the first bending mode of a wall leaf between two adjacent studs and the higher resonance frequency f_+ is the root mean square sum of f_0 and f_{mam} . The situation is more complicated when the two wall leaves are different, and the resonance frequencies are given by equation (12).

The frequency f_i is the resonance frequency of the first bending mode of the i th wall leaf between two adjacent studs. The problem is that the exact boundary conditions at the studs are not

known. If the boundary conditions were simply supported at each stud or guided at each stud, the resonance frequency f_i of the first bending mode of the i th wall leaf between two adjacent studs is

$$f_i = \frac{\pi}{2L^2} \sqrt{\frac{E_i h_i^2}{12\rho_i (1-\nu_i^2)}}, \quad (17)$$

where L is the spacing between the studs and E_i , ν_i , ρ_i and h_i are respectively the Young's modulus, the Poisson ratio, the density and the thickness of the i th wall leaf. Note that

$$m_i = \rho_i h_i \quad (18)$$

On the other hand, if the boundary conditions were clamped at each stud or free at each stud

$$f_i = \frac{3.56}{L^2} \sqrt{\frac{E_i h_i^2}{12\rho_i (1-\nu_i^2)}} \quad (19)$$

Equation (19) produces resonance frequency values which are 2.27 times greater than those given by equation (17). Because the wall leaves are vibrating out of phase in the effective mass-air-mass resonance mode, a rigid stud line connection will stop the wall leaves from moving at the line connection. Because the vibration of a wall leaf is symmetrical about the stud line connection in the effective mass-air-mass resonance mode, the part of the wall leaf on one side of the line connection will stop the part of the same wall leaf on the other side rotating at the line connection. Thus, the boundary conditions are likely to be close to clamped. As the studs become less rigid, the boundary conditions, imposed by the studs and the wall leaves on the other sides of the studs, are expected to depart further from clamped boundary conditions. Nightingale and Bosmans (1999) have shown experimentally that point connections of a building leaf to a stud behave like

line connections when their spacing is less than half the bending wave length of the building leaf. Thus, the above conclusions for line connections also apply to point connections in the low frequency region where the effective mass-air-mass resonance occurs. As the spacing between the point connections becomes greater than half the bending wavelength of the building leaf with increasing frequency, the behaviour of point connections gradually starts to differ from the behaviour of a line connection.

In this paper, the resonance frequency of the first bending mode between the studs is calculated by multiplying equation (17) for the simply supported resonance frequency by an empirical correction factor r . Japanese researchers (Masuda and Tanaka, 2018) use a similar approach to calculate the resonance frequencies of concrete floor slabs by multiplying the approximate formula for the resonance frequencies of a clamped panel by a frequency multiplier. The empirical correction factor r is determined by choosing the value which gives the best agreement between theory and experiment. It will be greater than zero and is expected to be less than 2.27. Unfortunately, this empirical correction factor r does vary between the different types of wall construction examined in this paper. An important output of this research is the value of this empirical correction factor r for a range of different wall constructions.

Because the vibration of the two wall leaves in the mass-air-mass resonance mode is out of phase there will be a surface through the studs where the studs are stationary. This means that the studs will not transmit any translational energy. Because the vibration of a wall leaf in the mass-air-mass resonance mode is symmetrical about the effective line connection between the stud and the wall leaf, the wall leaf will not rotate at the connection to the stud and hence will not transmit rotational energy. This conclusion applies regardless of the stiffness of the studs. This means that the leaves are effectively not coupled by the studs when vibrating in the mass-air-mass

resonance mode. Of course, the studs will transmit power for other types of leaf motion by coupling the motion of the wall leaves.

The critical frequency f_{ci} of the i th building element leaf is

$$f_{ci} = \frac{c^2}{2\pi} \sqrt{\frac{12\rho_i(1-\nu_i^2)}{E_i h_i^2}} \quad (20)$$

The experimental observation is that a building leaf consisting of two layers, which individually have same sheet material properties and thickness, and which is screwed or spot glued to the studs, has the same critical frequency as a single layer with the same sheet material properties and thickness. The reason is that the spot fastening enables the two layers to slide relative to each other when bent dynamically, provided the bending wave length is shorter than the screw spacing. In the sound insulation prediction method used in this paper, this behaviour is modelled by treating the double layers as a single layer with twice the thickness and one quarter of the Young's modulus of the actual single layer sheets. This means that the product $E_i h_i^2$ is the same for both the double layer and single layer building element leaves. Thus, these double and single layer leaves have the same critical frequencies and the same bending wave resonances between studs with the same spacing.

The theory used to predict the sound insulation of cavity stud building elements in this paper is that of Davy (2009; 2010; 2012). This theory uses the cavity width and the mass per unit area of each building element leaf to calculate the adiabatic mass-air-mass resonance frequency. In order to replace this frequency with the upper resonance frequency f_+ , the adiabatic mass-air-mass resonance frequency equation (the last two expressions in equation (16)) is inverted and used

215 to calculate the equivalent cavity width d_{eq} which would make the adiabatic mass-air-mass
 216 resonance frequency equal to the upper resonance frequency f_+ .

$$217 \quad d_{eq} = \rho_0 \frac{m_1 + m_2}{m_1 m_2} \left(\frac{c}{2\pi f_+} \right)^2 \quad (21)$$

218 This equivalent cavity width is used instead of the actual cavity width when applying the existing
 219 theory of Davy (2009; 2010; 2012) in order to avoid reprogramming the existing theory.

220 All the cavity stud walls considered in this paper had porous sound absorbing material in
 221 their wall cavities. The effect of the porous sound absorbing material in the cavity is modelled as
 222 the sound absorption coefficient of the cavity sides of the wall leaves following the approach of
 223 Mulholland *et al.* (1967). Based on the observations of Narang (1993) and Davy *et al.* (2017) that
 224 adding porous sound absorbing material to a wall cavity changes the speed of sound from the
 225 adiabatic value to the isothermal value, the isothermal speed of sound was used in equation (15).
 226 Note however that the adiabatic speed of sound is used in equation (21). For 25 gauge studs, it
 227 appears experimentally that the decrease due to the isothermal speed of sound in wall cavities filled
 228 with sound absorbing material counteracts the smaller increase in the mass-air-mass resonance
 229 frequency due to the drum mode.

230 One difference from Davy (2009), is that because all the wall cavities of the walls
 231 considered in this paper contain sound absorbing material, the sound absorption coefficient α of
 232 the wall cavity is set equal to the maximum value given by equation (35) of Davy (2009). However,
 233 because the theory could not predict some of the very deep dips in the sound insulation spectrum
 234 at the upper resonance frequency f_+ , in some cases the sound absorption coefficient of the wall
 235 cavity is multiplied by a factor B at and below a frequency f_B . The empirical values B and f_B are

determined by making the theory agree with experiment as well as possible. The values of this factor B and the upper frequency f_B at which it is used are important outputs of this paper.

$$\alpha = \begin{cases} Dkd_{eq} & \text{if } kd_{eq} < 1 \\ D & \text{if } kd_{eq} \geq 1 \end{cases} \quad (22)$$

$$D = \begin{cases} B & \text{if } f \leq f_B \\ 1 & \text{if } f > f_B \end{cases} \quad (23)$$

$$0 < B \leq 1 \quad (24)$$

k is the wavenumber of sound in air. Another difference from Davy (2010) and Davy (2012) is that sound transmission between the wall leaves via the studs is included below the resonance frequency.

A. Review of Davy's sound insulation theory

The sound insulation theory used in this paper (Davy, 2009; Davy, 2010; Davy, 2012) assumes that the sound transmission via the air in the wall cavity and the sound transmission via the studs can be predicted separately and added together to obtain the actual sound transmission. Both wall leaves and the air cavity are assumed to be of infinite lateral extent.

For sound transmission via the air cavity, the studs are assumed to have no effect on the air cavity or on the vibration and sound radiation of the wall leaves. This assumption works well because the reduction of the airborne induced vibration of the wall leaves caused by the studs appears to be cancelled out by the increase in radiation efficiency due to the presence of the studs. Only the forced vibration of the wall leaves is included when calculating the radiated sound power

below the critical frequency due to the airborne induced vibration because the radiation efficiency of the resonant vibration is so much lower.

Below $2/3$ of the mass-air-mass resonance frequency, the sound insulation of the wall is modelled as though it is a single leaf wall with the same total mass per unit area. The angular dependent mass law is integrated over angle of incidence up to a frequency and size dependent limiting angle to account for the effect of the actual finite size of the panel on the radiation efficiency (Sewell, 1970).

Between the mass-air-mass resonance frequency and the critical frequency, the angular dependent air borne sound transmission via the cavity is calculated using equation (C-10) of Rudder (1985) which is derived using the approach of Mulholland *et al.* (1967). This equation models the sound absorption in the cavity as a sound absorption coefficient of the cavity sides of the wall leaves. This equation is approximated by assuming that its value is that which occurs at the oblique mass-air-mass resonance angle of incidence. This assumption is fine when the wall cavity contains sound absorbing material. For an empty wall cavity, a sound absorption coefficient which is greater than the actual physical sound absorption coefficient of the wall leaves needs to be used to counteract the effects of this assumption. The angular dependent air borne sound transmission is integrated up to the maximum of Sewell's (1970) variable limiting angle and 61.4° . The 61.4° is chosen to make the theory agree with Sharp's (Sharp, 1973; 1978; Sharp *et al.*, 1980) theory. At low frequencies, the cavity sound absorption coefficient is limited as indicated in equations (22) to (24). The sound transmission via the wall cavity between $2/3$ of the mass-air-mass resonance frequency and the mass-air-mass resonance frequency is calculated by interpolation.

When the frequency is greater than the lower of the critical frequencies of the two wall leaves, a method similar to that used by Cremer (1942) is followed. This approach assumes that most of the sound transmission occurs at angles of incidence close to the coincidence angle and that the critical frequencies are not too different. It extends Cremer's method by only integrating over angles of incidence from 0 to 90 degrees rather than extending the limits to plus and minus infinity in order to make integration easier as Cremer did. It also uses the resonant radiation impedance for a finite size panel rather than that for an infinite size panel. This resonant radiation impedance is set equal to one above the lower of the critical frequencies of the two wall leaves. Between 0.9 times and 1 times the lower of the two critical frequencies the resonant radiation impedance is interpolated. Below the critical frequency, the maximum resonant transmission is assumed to occur at grazing angles of incidence, and the resonant transmission predicted by this approach is combined with the forced transmission predicted as described above to model the increase of sound transmission as the critical frequency is approached from below

The stud borne sound transmission of the cavity wall is modelled using Heckl's (1959a; b) theory for sound radiation of a panel due to point and line excitation. For line connections, it is assumed that all the vibration propagation in the wall leaves is normal to the line connections. The theory differs from Sharp's theory (Sharp, 1973; 1978; Sharp *et al.*, 1980) by integrating over the angle of incidence of the exciting diffuse field sound instead of dividing the mass per unit area of the wall leaves by 1.9, and by replacing Sharp's empirical correction factor of 5 dB with the effects of the resonant vibration of the wall leaves. This paper also extends the theory to frequencies at and above the critical frequencies of the wall leaves and allows the connections to be modelled as four pole networks. It differs from Vigran's theory (2010a; b) by assuming that the frequency is small compared to the critical frequency when calculating the radiation of an infinite version of

the second wall leaf due to the structural connection acting on it and correcting for this by including the resonant radiation of the finite version of the wall leaf. The resonant radiation efficiency is limited to a maximum value of one. Wood studs are assumed to be rigid and massless. Steel studs are assumed to be massless translational springs whose stiffness varies with frequency. The line connection theory is asymmetrical with regard to the critical frequencies and the damping loss factors of the wall leaves. This is partially solved by requiring the calculation to be made in the direction from the wall leaf with the lower critical frequency towards the wall leaf with the higher critical frequency. However, as Heckl pointed out in a personal communication with the first author, it is still asymmetrical with regard to the damping loss factors of the wall leaves. This is solved by using the average of the damping loss factors for both wall leaves.

III. THE EQUIVALENT TRANSLATIONAL COMPLIANCE OF STEEL STUDS

The equivalent translational compliance of a steel stud frame and the method that fastens the wall leaves to the steel stud frame is the compliance of translational line springs spaced at the stud spacing distance for the line connection model, or the compliance of translational point springs for the point connection model, which transfer the same amount of vibrational power between the two wall leaves as the steel stud frame and the method that fastens the wall leaves to the steel stud frame. The number of translational point springs per unit area is equal to the number of connections per unit area between the steel stud frame and a wall leaf. The equivalent translation compliance for the line connection model has dimensions of length per (force per unit length) giving dimensions of length squared per unit force or the inverse of pressure. For the point connection model, the dimensions of the equivalent translational compliance are length per unit force. The power transmitted by the actual steel stud frame between the wall leaves can be transmitted by

both translational motion and rotational motion.

This section gives the equivalent translational compliance of 92 mm deep C-section steel studs empirically derived by Davy *et al.* (2018) for use in sound insulation prediction models. The equivalent translational compliance C_M is a function of the frequency f , the number of point connections per unit area n or the stud spacing b , the reduced surface density m_r , the sheet steel gauge g and the area S of the test wall. The reduced surface density is

$$m_r = \frac{m_1 m_2}{m_1 + m_2}. \quad (25)$$

TABLE I. The thickness in mm of different gauges of sheet steel according to different authors.

Gauge g	Dong and Loverde (2015)	Quirt <i>et al.</i> (1995)	Poblet-Puig <i>et al.</i> (2009)	Nash (2006)
26		0.45 mm		0.551 mm
25	0.41 mm	0.53 mm	0.47 mm	0.6274 mm
20 equivalent	0.58 mm			
20	0.91 mm			
18	1.17 mm	1.22 mm		
16	1.45 mm	1.52 mm		

It is used because it is how the two surface densities are combined in the equation used to calculate the normal incidence mass-air-mass resonance frequency of the cavity wall. The thickness in mm of different gauges of sheet steel according to different authors is given in TABLE I. The actual measured thickness in mm of the steel studs in the walls which are analysed in this paper are those

in the second column of TABLE I. It should be noted that there is quite a range of thicknesses in mm for a given gauge in TABLE I, especially for the thinner higher gauge number sheet steel. The 20 gauge equivalent studs are made from steel thinner than 20 gauge, and are marketed by the manufacturer as having the same strength and other structural properties as 20 gauge studs.

TABLE II. Values and confidence limits for the constants in the low and high frequency range for the line connection model.

Frequency Range	Constant	Value	95% Upper limit	95% Lower limit
63 to 250 Hz	A (1/Pa)	6.07×10^{-4}	2.67×10^{-3}	1.38×10^{-4}
	x_f	-1.040	-0.903	-1.178
	x_m	-1.40	-1.16	-1.65
	x_g	0.666	1.084	0.249
250 to 5000 Hz	A (1/Pa)	2.58×10^{-4}	4.38×10^{-4}	1.52×10^{-4}
	x_f	-1.52	-1.49	-1.54
	x_m	-1.12	-1.03	-1.21
	x_b	-0.257	-0.134	-0.379
	x_g	1.52	1.67	1.37

The empirical equations for the equivalent translational compliance C_M are

$$C_M = A \left(\frac{f}{f_0} \right)^{x_f} \left(\frac{m_r}{m_{r0}} \right)^{x_m} \left(\frac{b}{b_0} \right)^{x_b} \left(\frac{g}{g_0} \right)^{x_g} \left(\frac{S}{S_0} \right)^{x_s} \quad (\text{Line connection}) \quad (26)$$

and

$$C_M = A \left(\frac{f}{f_0} \right)^{x_f} \left(\frac{m_r}{m_{r0}} \right)^{x_m} \left(\frac{n}{n_0} \right)^{x_n} \left(\frac{g}{g_0} \right)^{x_g} \left(\frac{S}{S_0} \right)^{x_S} \quad (\text{Point connection}). \quad (27)$$

TABLE III. Values and confidence limits for the constants in the low and high frequency range for the point connection model.

Frequency Range	Constant	Value	95% Upper limit	95% Lower limit
63 to 250 Hz	A (m/N)	4.06×10^{-5}	7.11×10^{-4}	2.32×10^{-6}
	x_f	-0.760	-0.493	-1.026
	x_m	-1.96	-1.48	-2.44
	x_g	1.68	2.49	0.64
250 to 5000 Hz	A (m/N)	4.94×10^{-7}	2.15×10^{-6}	1.14×10^{-7}
	x_f	-1.16	-1.10	-1.21
	x_m	-1.18	-0.97	-1.39
	x_n	0.747	1.042	0.452
	x_g	2.49	2.87	2.11
	x_S	0.355	0.550	0.159

A is a constant, f is the frequency, f_0 is 1 Hz, m_r is the reduced surface density, m_{r0} is 1 kg/m², b is the distance between the line connections (stud spacing), b_0 is 1 m, n is the number of point connections per unit area calculated from the stud spacing and the screw spacing, n_0 is 1 1/m², g is the gauge of the sheet steel used to manufacture the steel studs, g_0 is 1, S is the area of the wall and S_0 is 1 m². The constant A has units of 1/Pa for line connections and m/N for point connections. The symbols x_f , x_m , x_g , x_S , x_b , or x_n are dimensionless exponent constants. The values

and 95% confidence limits of A and the dimensionless exponent constants are given in TABLE II for the line connection model and in TABLE III for the point connection model. If a dimensionless exponent constant does not appear in the applicable Table for a particular frequency range and model, the factor involving it is not used for that particular frequency range and model.

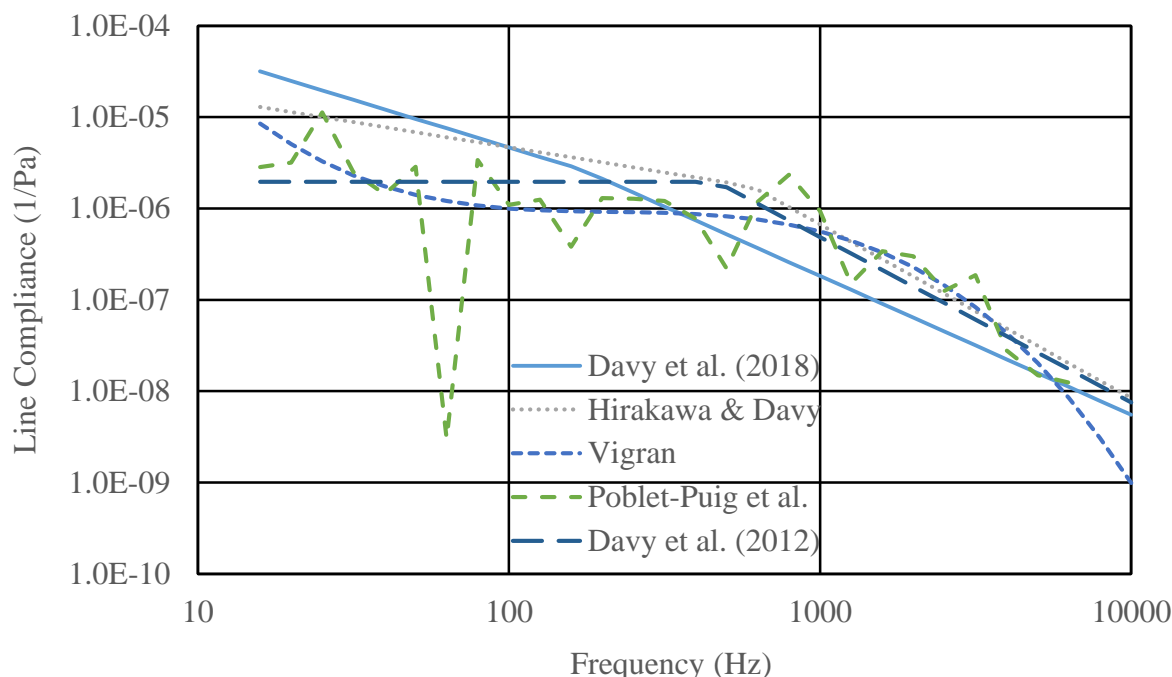


FIG. 1. (Color online) The line compliance of nominal 25 gauge steel studs, with gypsum plaster board leaves with a reduced surface density of 4.9 kg/m^2 , a stud spacing of 0.6 m and a stud width of 70 mm, derived by Davy et al. (2018), Hirakawa and Davy (2015), Vigran (2010a), Poblet-Puig et al. (2009) and Davy et al. (2012).

FIG. 1 compares the line compliance of nominal 25 gauge steel studs, with gypsum plaster board leaves with a reduced surface density of 4.9 kg/m^2 , a stud spacing of 0.6 m and a stud width of 70 mm, derived by Davy et al. (2018) with that derived by Hirakawa and Davy (2015), Vigran (2010a), Poblet-Puig et al. (2009) and Davy et al. (2012). FIG. 2 compares the point compliance of nominal 25 gauge steel studs, with gypsum plaster board leaves with a reduced surface density

of 4.9 kg/m², with 5.4 point connections per square metre and a specimen area of 7.4 m². derived by Davy et al. (2018) with that derived by Hirakawa and Davy (2015). There is rough agreement between these compliances derived by different authors.

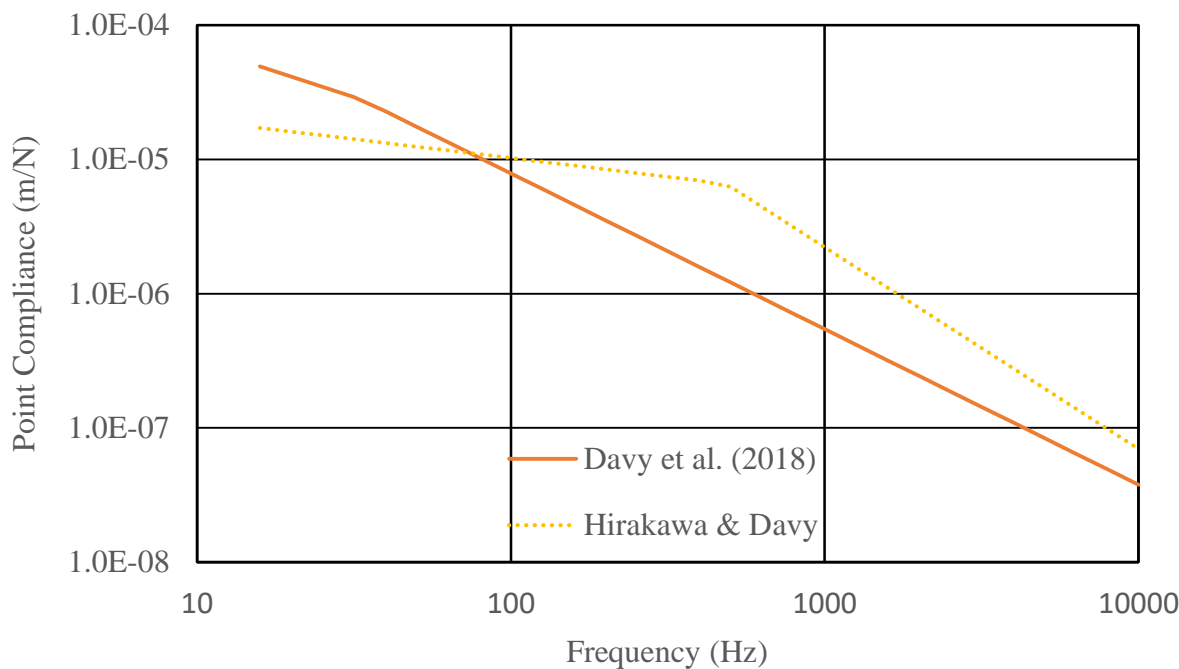


FIG. 2. (Color online) The point compliance of nominal 25 gauge steel studs, with gypsum plaster board leaves with a reduced surface density of 4.9 kg/m², with 5.4 point connections per square metre and a specimen area of 7.4 m² derived by Davy et al. (2018) with that derived by Hirakawa and Davy (2015).

IV. RESULTS

The empirically determined bending wave resonance frequency multiplier and sound absorption coefficient multiplier for 92 mm steel stud cavity walls, with layers of 16 mm gypsum plaster board (GPB) on each side, measuring 3.66 m wide by 4.57 m high are given in Table IV.

Table IV. Empirically determined bending wave resonance frequency multiplier and sound absorption coefficient multiplier for 92 mm steel stud cavity walls, with layers of 16 mm gypsum plaster board (GPB) on each side, measuring 3.66 m wide by 4.57 m high. The maximum frequency for the application of the sound absorption multiplier is also given.

Gauge g	Spacing b (m)	GPB Layers	GPB Layers	Frequency Multiplier r	Absorption Multiplier B	Upper Frequency f_B (Hz)
16	0.4064	2	2	1.7	0.4	160
16	0.4064	2	1	1.7	0.4	160
16	0.4064	1	1	1.7	0.4	160
16	0.6096	2	2	1.7	1	0
16	0.6096	2	1	1.7	1	0
16	0.6096	1	1	1.7	1	0
18	0.4064	2	2	1.3	0.5	160
18	0.4064	2	1	1.3	0.5	160
18	0.4064	1	1	1.3	0.7	160
18	0.6096	2	2	1.7	1	0
18	0.6096	2	1	1.7	1	0
18	0.6096	1	1	1.3	1	0
20	0.4064	2	2	1.3	0.5	160
20	0.4064	2	1	1.3	0.6	160
20	0.4064	1	1	1.3	0.6	160
20	0.6096	2	2	1.7	1	0
20	0.6096	2	1	1.7	1	0
20	0.6096	1	1	1.7	1	0
20E	0.4064	2	2	1.3	1	0
20E	0.4064	2	1	1.3	1	0
20E	0.4064	1	1	1.3	1	0
20E	0.6096	2	2	1.7	1	0
20E	0.6096	2	1	1.7	1	0
20E	0.6096	1	1	1.3	1	0
25	0.4064	2	2	1	1	0
25	0.4064	2	1	1	1	0
25	0.4064	1	1	1	1	0
25	0.6096	2	2	1	0.6	80
25	0.6096	2	1	1	0.6	80
25	0.6096	1	1	1	0.15	63

Table V. Empirically determined bending wave resonance frequency multiplier and sound absorption coefficient multiplier for 92 mm steel stud cavity walls, with layers of 16 mm gypsum plaster board (GPB) on each side, measuring 3.66 m wide by 2.44 m high. The maximum frequency for the application of the sound absorption multiplier is also given.

Gauge g	Spacing b (m)	GPB Layers	GPB Layers	Frequency Multiplier r	Absorption Multiplier B	Upper Frequency f_B (Hz)
16	0.4064	2	2	1.3	0.7	160
16	0.4064	2	1	1.3	0.7	160
16	0.4064	1	1	1.3	0.7	160
16	0.6096	2	2	1.7	0.5	80
16	0.6096	2	1	1.3	0.5	80
16	0.6096	1	1	1.3	0.5	80
20	0.4064	2	2	1.3	0.6	160
20	0.4064	2	1	1.3	0.6	160
20	0.4064	1	1	1.3	0.6	160
20	0.6096	2	2	1.7	0.6	100
20	0.6096	2	1	1.3	0.6	100
20	0.6096	1	1	1.3	0.6	80
25	0.4064	2	2	0.8	1	0
25	0.4064	2	1	0.6	0.8	125
25	0.4064	1	1	0.6	0.8	125
25	0.6096	2	2	0.6	0.4	80
25	0.6096	2	1	0.6	0.6	80
25	0.6096	1	1	0.6	0.6	80

The maximum frequency for the application of the sound absorption multiplier is also given in Table IV. The same information for 92 mm steel stud cavity walls measuring 3.66 m wide by 2.44 m high is given in Table V. The steel stud wall data is taken from B  tit (2010), Loverde et al. (2012) and Dong and Loverde. (2015). This is the same data that was used to derive the steel stud line and point compliances given in section III.

Table VI. Empirically determined bending wave resonance frequency multiplier and sound absorption coefficient multiplier for 39 x 89 mm wood stud cavity walls, with layers of 13 or 16 mm gypsum plaster board (GPB) on each side, measuring 3.05 m wide by 2.44 m high. The maximum frequency for the application of the sound absorption multiplier is also given. The numbers in the GPB Layers columns denote the thicknesses of the GPB layers in mm. The letter X denotes type X fire rated GPB.

GPB Layers	GPB Layers	Frequency Multiplier r	Absorption Multiplier B	Upper Frequency f_B (Hz)
13X	13X	1.9	0.3	160
13	13	1.5	0.3	125
13X	13X	1.7	0.3	125
16X	16X	1.4	0.3	160
13X	13X+13X	1.7	0.3	160
13	13+13	1.7	0.2	125
16X	16X+16X	1.5	0.3	160
13X+13X	13X+13X	1.7	0.3	160

Table VI gives the same information for 8 cavity walls, with 39 x 89 mm wood studs and layers of 13 or 16 mm gypsum plaster board (GPB) on each side, measuring 3.05 m wide by 2.44 m high. The numbers in the GPB Layers columns denote the thicknesses of the GPB layers in mm.

The letter X denotes type X fire rated GPB. The wood stud wall data is taken from Halliwell et al. (1998) and experimentally determined values of Young's modulus and surface density were used. Quirt *et al.* (1995) determined the Young's modulus by supporting beams of gypsum plaster board horizontally on pipe supports with a 2.5 cm overhang at both ends. The beams were tapped with an impact hammer or a finger and the impulse response at the centre of the beam was measured with an accelerometer. The impulse response was Fourier transformed to obtain the frequency response. The frequency of the first beam mode was determined from the first resonance frequency peak in the frequency response and the Young's modulus was calculated by assuming that the beam was simply supported.

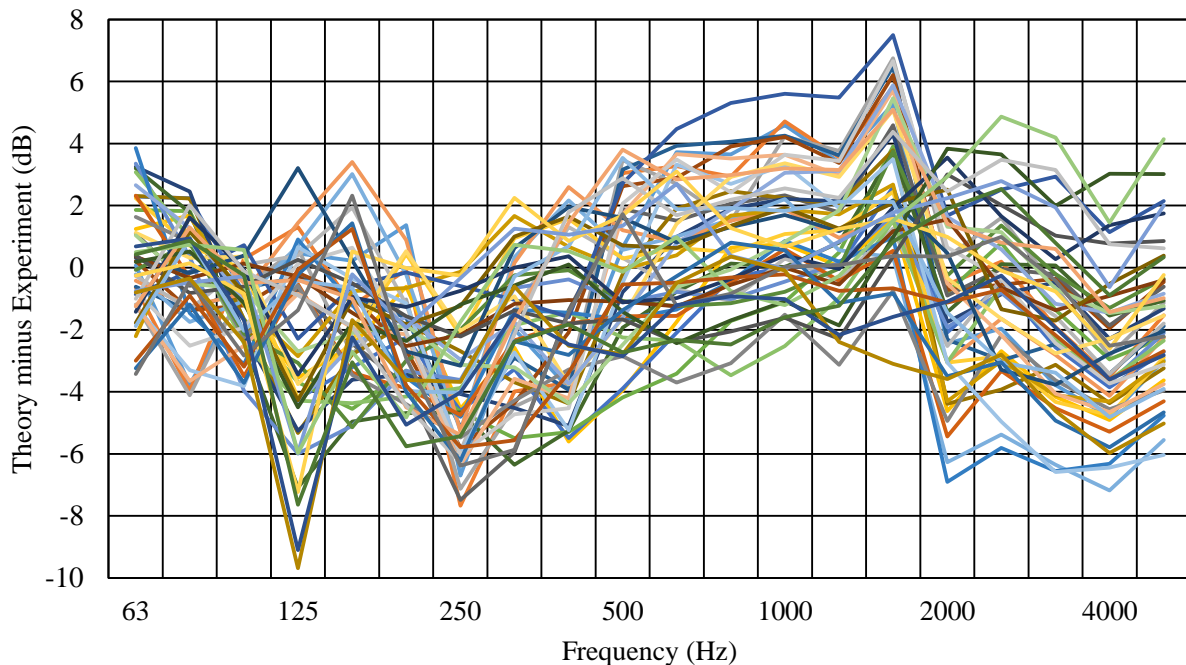


FIG. 3. (Color online) The difference in sound insulation between the theoretical prediction using the line connection model and the experimental measurement for 92 mm steel stud cavity walls, with layers of 16 mm gypsum plaster board on each side.

For the six 16 gauge steel stud walls with a height of 4.57 m, multiplying the simply supported resonance frequency by an frequency multiplier r of 1.7 worked well. This frequency multiplier r was also good for the higher walls with 18 gauge and equivalent 20 gauge studs spaced at 610 mm with two layers of 16 mm GPB on each side or with two layers on one side and one layer on the other side. The other 18 gauge and equivalent 20 gauge stud walls needed a frequency multiplier r of only 1.3. Frequency multipliers r of 1.7 and 1.3 were used for the higher 20 gauge stud walls with stud spacings of 610 mm and 406 mm respectively. The higher 25 gauge stud walls needed a frequency multiplier r of only 1.

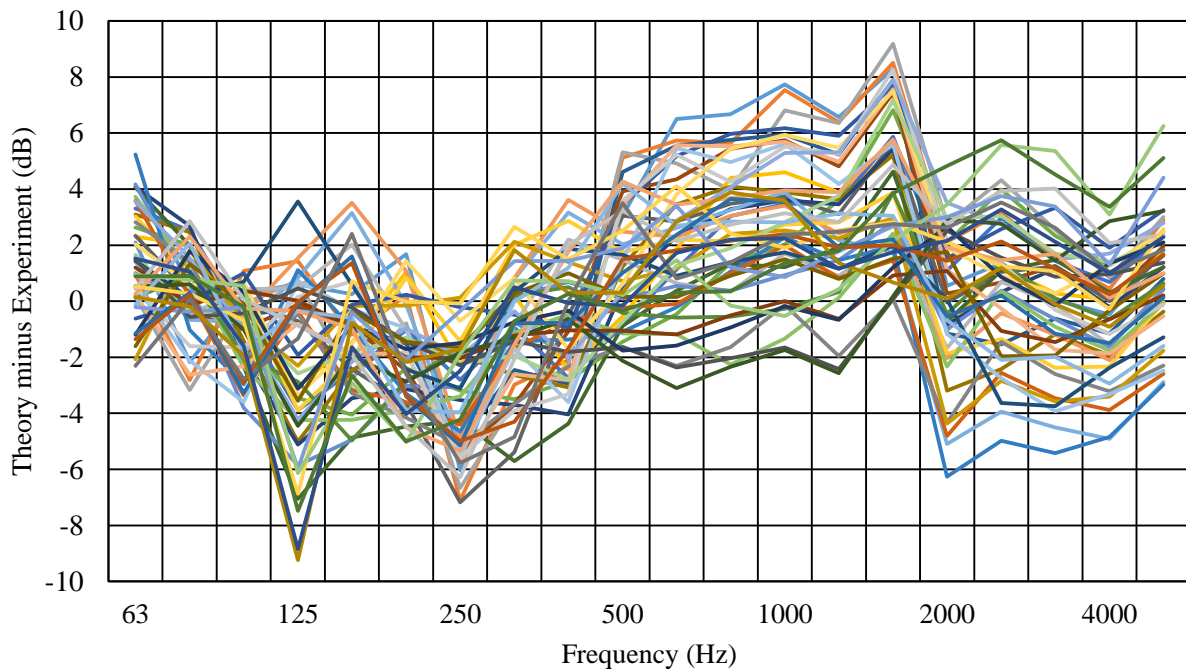


FIG. 4. (Color online) The difference in sound insulation between the theoretical prediction using the point connection model and the experimental measurement for 92 mm steel stud cavity walls, with layers of 16 mm gypsum plaster board on each side.

A frequency multiplier r of 1.3 was used for the lower height 16 and 20 gauge stud walls except for the two walls with a stud spacing of 610 mm and two layers of GPB on each side of the

studs which both used a frequency multiplier r of 1.7. The lower height 25 gauge stud walls needed a frequency multiplier r of 0.6 except for the wall with a stud spacing of 406 mm and two layers of GPB on each side which required a frequency multiplier of 0.8. Thus, the general trend was for the frequency multiplier r to decrease as the stud gauge increased, as the reduced mass decreased and as the stud spacing decreased. It is interesting to note that for the resonance frequencies of concrete floor slabs, Japanese researchers (Masuda and Tanaka, 2018) use the approximate formula for the resonance frequencies for a clamped panel with a frequency multiplier of 0.8. This is the same as a frequency multiplier of 1.8 times the simply supported panel resonance frequencies.

For the eight wooden stud walls, the frequency multiplier r varied between 1.4 and 1.9 with no obvious pattern, although the frequency multiplier r was 1.7 for half of the walls. For these wooden stud walls the absorption multiplier B was 0.3 for seven of the walls and 0.2 for the other wall. The maximum frequency of application f_B of the absorption multiplier was 160 Hz for five of the walls and 125 Hz for the three other walls. There was a tendency for the walls with the highest reduced mass to have the higher maximum frequency of application.

For the steel stud walls, the absorption multiplier B varied between 0.4 and 1 except for one value B of 0.15. The absorption multiplier B was different from 1 for all but one of the lower height walls. For the higher steel stud walls, the absorption multiplier B was different from 1 for the 16, 18 and 20 gauge walls with a stud spacing of 406 mm and the maximum frequency of application f_B was 160 Hz for these walls. The situation was reversed for the higher height 25 gauge steel stud walls and the absorption multipliers B were different from 1 for the 610 mm stud spacings and the maximum frequency of application f_B was 80 Hz for the two heavier walls and 63 Hz for the lighter wall.

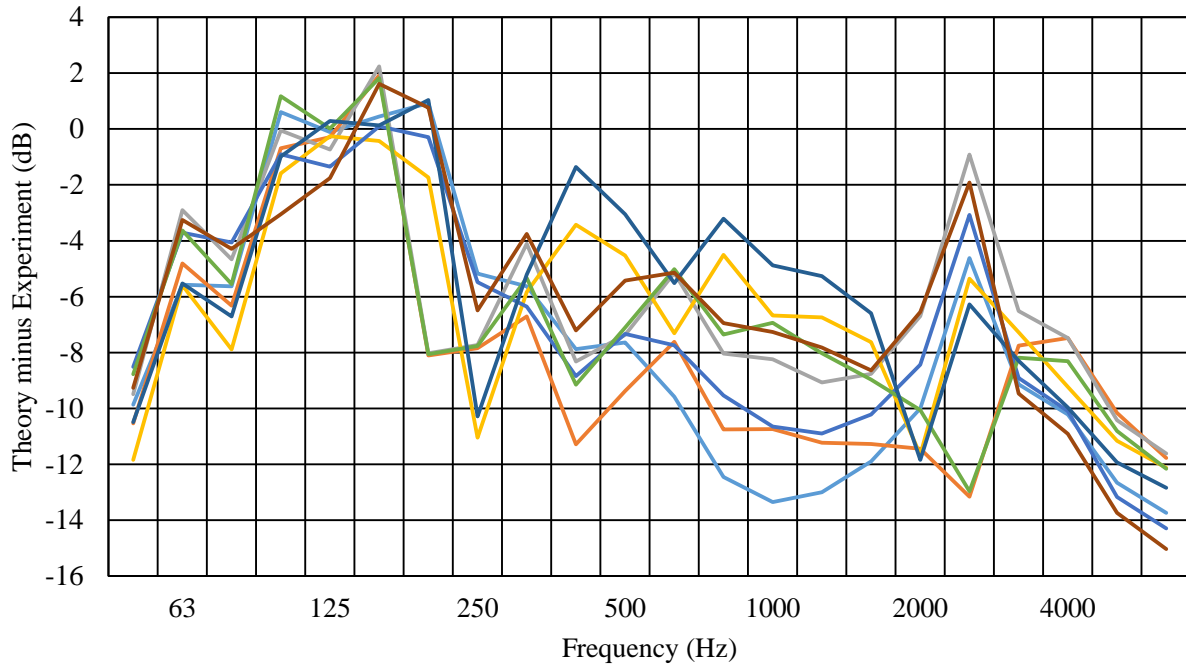


FIG. 5. (Color online) The difference in sound insulation between the theoretical prediction using the line connection model and the experimental measurement for 39 x 89 mm wood stud cavity walls, with layers of 13 or 16 mm gypsum plaster board on each side.

FIG. 3 and FIG. 4 show the differences between the predicted sound insulation and the experimentally measured sound insulation for the line compliance model and the point compliance model respectively for the steel stud walls. The point compliance model gives slightly more spread of differences than the line compliance model. The spread of differences at and above the critical frequency is believed to be because the different walls have a range of in situ damping loss factor values compared to the value of 0.03 assumed in this paper.

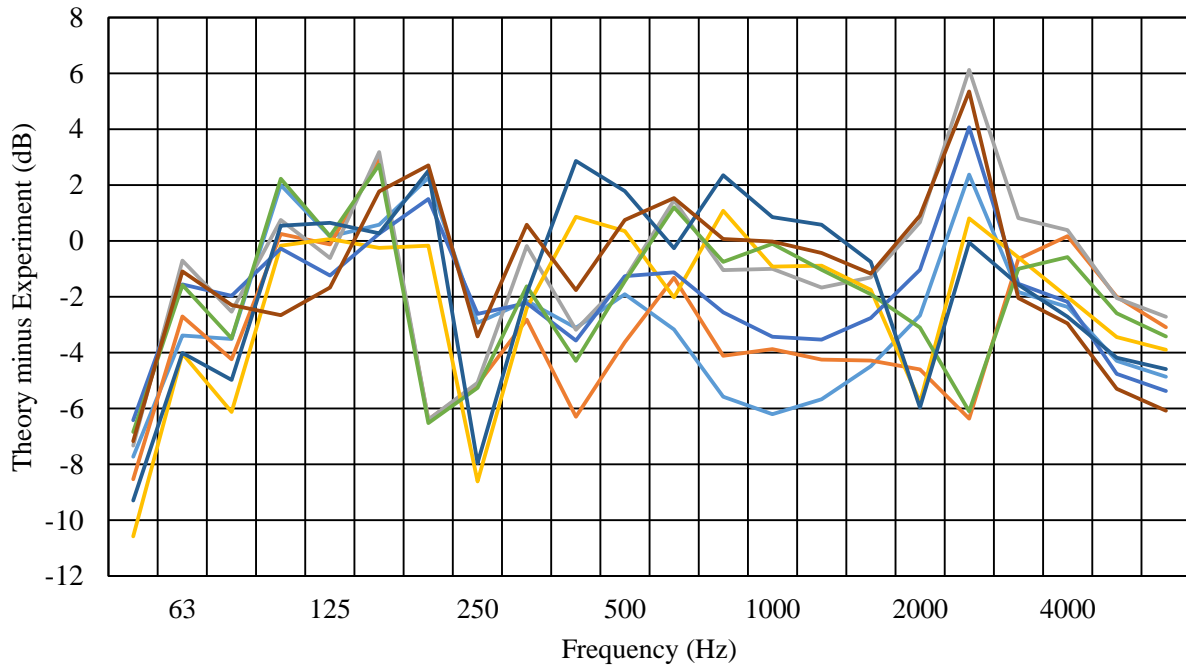


FIG. 6. (Color online) The difference in sound insulation between the theoretical prediction using the point connection model and the experimental measurement for 39 x 89 mm wood stud cavity walls, with layers of 13 or 16 mm gypsum plaster board on each side.

FIG. 5 and FIG. 6 show the differences between the predicted sound insulation and the experimentally measured sound insulation for the line compliance model and the point compliance model respectively for the wood stud walls. FIG. 5 shows, as Davy (2012) commented, that above 200 Hz the line connection model underestimates the sound insulation of the wood stud building elements. Presumably a similar under prediction would occur for steel stud building elements if the empirically determined line compliance did not automatically include a correction for this difference because of the way it was derived. Applying the empirical corrections presented in this paper has led to the under prediction of the sound insulation of the wood stud building elements in the frequency range below 100 Hz.

There are still large differences between theory and experiment at some frequencies. One of the reasons for this is the very rapid increase in the experimental sound insulation immediately above the effective normal incident mass-air-mass resonance frequency, which the simple theory used in this paper cannot reproduce. Another reason is the very rapid decrease in the experimental sound insulation as the critical frequency is approached from below. Again, simple sound insulation theories cannot predict this rapid decrease.

There is also a big variation in the difference between theory and experiment above the critical frequency. This is believed to be due to a large variation in the in-situ damping loss factor between different building element specimens compared to the value of 0.03 assumed in this paper, although on average the 0.03 value for the damping loss factor appears to be correct.

V. CONCLUSION

This paper presents the theory for calculating the effective normal incident mass-air-mass resonance frequency for a double leaf cavity stud building element. If the two building element leaves are similar, this frequency is the root mean square of the first bending wave mode resonance frequency of the building element leaf between adjacent studs and the normal incident mass-air-mass resonance frequency of the version of the building element without studs. If the building element cavity contains porous sound absorbing material, the isothermal normal incident mass-air-mass resonance frequency should be used. Although not shown in this paper, for a building element cavity without porous sound absorbing material, it is expected that the adiabatic normal incident mass-air-mass resonance frequency should be used.

Because the exact boundary conditions of the building element leaves at the studs are not known, and because these boundary conditions will depend on the compliance of the studs, this

paper gives empirically determined factors by which to multiply the first bending wave mode resonance frequency of the building element leaf between adjacent studs with simply supported boundary conditions in order to obtain this resonance frequency with the actual boundary conditions.

In order to calculate the correct sound insulation of a double leaf cavity stud building element with porous sound absorbing material in its cavity in the vicinity of the effective normal incident mass-air-mass resonance frequency, this paper gives empirically determined factors by which the assumed sound absorption coefficient of the cavity must be multiplied and the empirically determined frequency up to and including which this multiplication factor must be used.

This paper also gives empirically derived equations for the equivalent translational line and point compliances of steel studs manufactured from different sheet steel gauges. It compares these equations for the case of 25 gauge steel studs with earlier research.

The range of differences between theory and experiment for the sound insulation of cavity stud building elements with porous sound absorbing material in their cavities have been significantly reduced in the region of the effective normal incident mass-air-mass resonance frequency but is still large across the whole frequency range.

REFERENCES

Bétit, A. (2010). "Performance details of metal stud partitions," Sound and Vibration **March 2010**, 14-16.

Bradley, J. S. (2002). "IBANA-Calc Validation Studies," in *Institute for Research in Construction Research Report IRC RR-125* (National Research Council of Canada), p.

522 50.

523 Bradley, J. S., and Birta, J. A. (2000). "Laboratory measurements of the sound insulation of
524 building façade elements," in *Institute for Research in Construction Internal Report IRC*
525 *IR-818* (National Research Council of Canada, Ottawa), p. 183.

526 Bradley, J. S., and Birta, J. A. (2001). "On the sound insulation of wood stud exterior walls," J.
527 Acoust. Soc. Am. **110**, 3086-3096.

528 Bradley, J. S., Lay, K., and Norcross, S. G. (2002). "Measurements of the sound insulation of a
529 wood framed house exposed to aircraft noise," in *Institute for Research in Construction*
530 *Internal Report IRC IR-831* (National Research Council of Canada, Ottawa), p. 113.

531 Cremer, L. (1942). "Theorie der Schalldämmung Wände bei schrägem Einfall, Akustische,"
532 Zeitschrift **7**, 81–104.

533 Davy, J. L. (2009). "Predicting the sound insulation of walls," Build. Acoust. **16**, 1-20.

534 Davy, J. L. (2010). "The improvement of a simple theoretical model for the prediction of the
535 sound insulation of double leaf walls," J. Acoust. Soc. Am. **127**, 841-849.

536 Davy, J. L. (2012). "Sound transmission of cavity walls due to structure borne transmission via
537 point and line connections," J. Acoust. Soc. Am. **132**, 814–821.

538 Davy, J. L., Debevc, M., and Blanc, C. (2017). "The sound insulation autoclaved aerated
539 concrete panels lined with gypsum plaster board," in *Inter-noise 2017* (I-INCE, Hong
540 Kong, China), pp. 3879-3889.

541 Davy, J. L., Fard, M., Dong, W., and LoVerde, J. (2018). "The equivalent translational
542 compliance of steel studs with different steel gauge thicknesses," in *Inter-noise 2018*
543 (Chicago, USA), p. 12.

544 Davy, J. L., Guigou-Carter, C., and Villot, M. (2012). "An empirical model for the equivalent

545 translational compliance of steel studs," J. Acoust. Soc. Am. **131**, 4615–4624.

546 Dong, W., and Loverde, J. (2015). "Analysis of the effects on transmission loss of changes to
547 stud gauge, spacing, and height in single steel stud walls," in *Inter-noise 2015* (INCE
548 USA, San Francisco, USA), p. 10.

549 Halliwell, R. E., Nightingale, T. R. T., Warnock, A. C. C., and Birta, J. A. (1998). "Gypsum
550 board walls: transmission loss data," in *Internal Report IRC-IR-761* (Institute for
551 Research in Construction, National Research Council of Canada, Ottawa, Canada), p.
552 370.

553 Heckl, M. (1959a). "Schallabstrahlung von Platten bei Punktförmiger Anregung (Sound radiation
554 of plates with point excitation)," *Acustica* **9**, 371-380.

555 Heckl, M. (1959b). "Untersuchungen über die Luftschalldämmung von Doppelwänden mit
556 Schallbrücken (Investigations on the airborne sound insulation of double walls with
557 sound bridges)," in *The Third International Congress on Acoustics*, edited by L. Cremer
558 (Elsevier Publishing Company, Stuttgart, Germany), pp. 1010-1014.

559 Hirakawa, S., and Davy, J. L. (2015). "The equivalent translational compliance of steel or wood
560 studs and resilient channel bars," J. Acoust. Soc. Am. **137**, 1647-1657.

561 Lin, G. F., and Garrelick, J. M. (1977). "Sound-transmission through periodically framed parallel
562 plates," J. Acoust. Soc. Am. **61**, 1014-1018.

563 Loverde, J., Dong, W., and Bétit, A. (2012). "Investigation into the acoustical performance of
564 single stud steel wall assemblies," in *Internoise 2012* (New York City, USA), p. 6.

565 Masuda, K., and Tanaka, H. (2018). "Prediction of heavy impact sound level using mode shape
566 function method," in *25th International Congress on Sound and Vibration* (International
567 Institute of Sound and Vibration, Hiroshima, Japan), pp. 1-8.

568 Mulholland, K. A., Parbrook, H. D., and Cummings, A. (1967). "The Transmission Loss of
 569 Double Panels," *Journal of Sound and Vibration* **6**, 324–334.

570 Narang, P. P. (1993). "Effect of fiberglass density and flow resistance on sound transmission loss
 571 of cavity plasterboard walls," *Noise Control Engineering Journal* **40**, 215-220.

572 Nash, A. (2006). "Resilient ceiling construction in residential buildings," in *4th Joint ASA/ASJ*
 573 *Meeting (152nd Meeting of ASA)* (Honolulu HI USA), pp. 1-15.

574 Nightingale, T. R. T., and Bosmans, I. (1999). "Vibration response of lightweight wood frame
 575 building elements," *Build. Acoust.* **6**, 289-308.

576 Poblet-Puig, J., Rodriguez-Ferran, A., Guigou-Carter, C., and Villot, M. (2009). "The role of
 577 studs in the sound transmission of double walls," *Acta Acust. Acust.* **95**, 555-567.

578 Quirt, J. D., Warnock, A. C. C., and Birta, J. A. (1995). "Sound transmission through gypsum
 579 board walls: Sound transmission results," in *Internal Report IRC-IR-693* (National
 580 Research Council of Canada, Ottawa, Canada), p. 83.

581 Rudder, F. F. J. (1985). "Airborne Sound Transmission Loss Characteristics of Wood-Frame
 582 Construction, General Technical Report, FPL-43," (Forest Products Laboratory, Forest
 583 Service, United States Department of Agriculture, Madison, Wisconsin, USA), pp. 1-27.

584 Sewell, E. C. (1970). "Transmission of Reverberant Sound through a Single-Leaf Partition
 585 Surrounded by an Infinite Rigid Baffle," *J.Sound Vib.* **12**, 21–32.

586 Sharp, B. H. (1973). "A study of techniques to increase the sound insulation of building
 587 elements," in *Wyle Laboratories Report WR 73-5, Wyle Laboratories Research Staff, El*
 588 *Segundo, California, distributed as PB-222 829, National Technical Information Service,*
 589 *United States Department of Commerce, Springfield, Virginia.*, pp. 1-227.

590 Sharp, B. H. (1978). "Prediction Methods for the Sound Transmission of Building Elements,"

591 Noise Control Eng. **11**, 53-63.

592 Sharp, B. H., Kasper, P. K., and Montroll, M. L. (1980). "Sound Transmission through Building
593 Structures - Review and Recommendations for Research," in *NBS-GCR-80-250, National*
594 *Bureau of Standards, United States Department of Commerce, Washington, D. C., .*
595 *Distributed as PB81-187072, National Technical Information Service, United States*
596 *Department of Commerce, Springfield, Virginia, pp. 1-144.*

597 Van den Wyngaert, J. C. E., Schevenels, M., and Reynders, E. P. B. (2018). "Predicting the
598 sound insulation of finite double-leaf walls with a flexible frame," *Appl. Acoust.* **141**, 93-
599 105.

600 Vigran, T. E. (2010a). "Sound insulation of double-leaf walls - allowing for studs of finite
601 stiffness in the transfer matrix scheme," *Appl. Acoust.* **71**, 616-621.

602 Vigran, T. E. (2010b). "Sound transmission in multilayered structures - Introducing finite
603 structural connections in the transfer matrix method," *Appl. Acoust.* **71**, 39-44.

604